ACS Macro Letters

Letter

pubs.acs.org/macroletters

Disentanglement of Linear Polymer Chains Toward Unentangled Crystals

Chuanfu Luo*[,†] and Jens-Uwe Sommer[†,‡]

[†]Leibniz-Institut für Polymerforschung Dresden e.V., Hohe Strasse 6, 01069 Dresden, Germany

[‡]Institut für Theoretische Physik, Technische Universität Dresden, Zellescher Weg 17, 01062 Dresden, Germany

ABSTRACT: Large scale and long time molecular dynamics simulations and primitive path analysis are used to investigate the disentanglement of long linear polymer chains during their crystallization from the melt state. In general, two competitive processes, a slow decrease of average entanglement length during cooling caused by stiffening of chains and a strong increase during crystallization, can be observed. In both homogeneous and heterogeneous nucleation, disentanglement occurs via forming folds from locally unentangled segments and continues in postcrystallization processes (slow reorganization), in particular, during annealing. Re-entanglement processes after melting are slow and can lead to memory effects in heating−recooling protocols such as self-seeding.

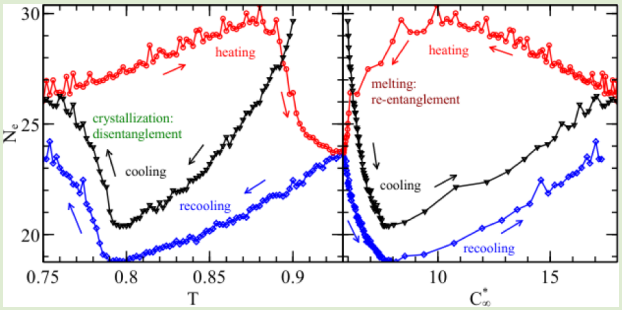

The understanding of polymer crystallization at a molecular level is one of the major unresolved problems of polymer science.[1−4] During cooling, stereoregular polymers display a spontaneous transition into a folded state. Crystallization from melts, except for short oligomers, is usually incomplete and results in the so-called semicrystalline state, where crystalline lamellae formed by folded chain parts coexist with amorphous regions. This is usually attributed to the nonequilibrium character of polymer crystals, which are assumed to be trapped in metastable states and cannot relax on experimental time scales. Although chemical details control the individual crystallization parameters, fundamental properties common to all polymers such as connectivity, local stiffness, and topological constraints should be responsible for a unique picture of the crystallization behavior of polymers.

As polymer chains shall be fully unentangled in ideal single crystals, crystallization of polymers from entangled melts is accompanied with an at least partial disentanglement process. The role of entanglements and possible scenarios of disentanglement during melt-crystallization has been debated in literature,[5−7] but experimental access to entanglement properties in semicrystalline polymers is difficult.[7,8] Although it is intuitive to relate the concept of entanglements with the frustration of a complete phase transformation or with memory effects such as observed in self-seeding experiments,[9,10] so far, no quantitative relations between entanglement properties and crystallization processes could be made. This is closely related to the problem of defining the state of entanglement of linear chains where topological properties such as knots and linking numbers are not well-defined. To define the topological state of a polymer melt, Everaers et al. have proposed an algorithm based on trajectories of Molecular Dynamics (MD) to analyze the Primitive Path (PP) of an entangled polymer chain, which allows quantitative insights to the entanglement properties of a certain structure.[11]

In this letter we report the application of Primitive Path Analysis (PPA)[11] to the local state of entanglement in dense polymers during various stages of crystallization and melting. Our results are based on our previous work where we have applied a coarse-graining poly(vinyl alcohol) (CG-PVA) model to simulate nucleation, growth, melting, and self-seeding processes of long chains.[12−14] We use a patched LAMMPS code,[15,16] and the details of our simulations are given in the caption of Figure 1. The results shown in this paper can be extended to other stereoregular flexible chains.

In Figure 1a, we show the changes of specific volume (v) during continuous cooling, heating, and recooling. The apparent crystallization temperature is T_c = 0.79 and 0.785 for cooling and recooling, respectively. The difference in T_c between cooling and recooling with same cooling rate shows that crystallization is dependent on the initial states.[7,8,17] The T_c is lower in recooling cycle, which seems to be counterintuitive because memory effects of the first crystallization cycle might facilitate the crystallization process and raise the apparent crystallization temperature.

As the specific volumes at melt state are the same for cooling and recooling, there must be some "hidden parameters" that lead to the difference in T_c of the two processes. These "hidden parameters" are usually crudely considered as thermal history. Among these "hidden parameters", the state of entanglement of chains should be considered. In principle, the state of

Received: October 19, 2012
Accepted: December 18, 2012
Published: December 21, 2012

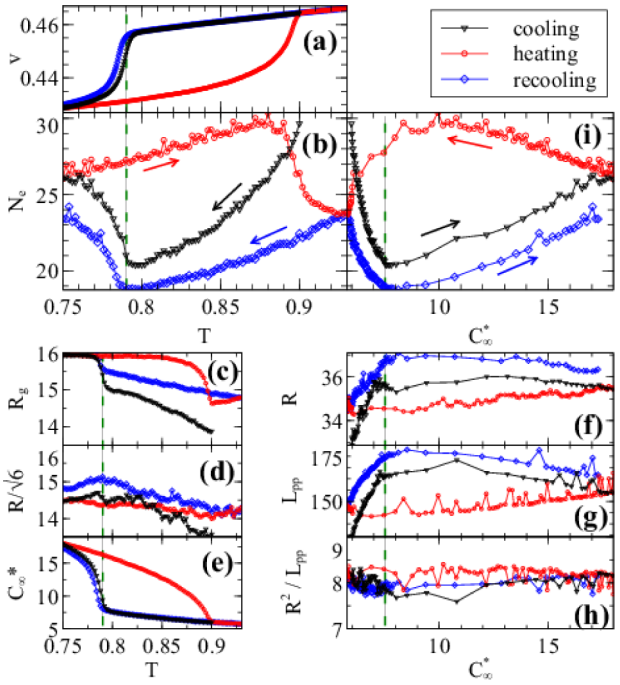

Figure 1. (a–e) Specific volume (v), entanglement length (N_e), radius of gyration (R_g), end-to-end distance (R), and effective persistence length ($C_\infty^* = (1 + \langle\cos\theta\rangle)/(1 - \langle\cos\theta\rangle)$, where θ is the angle between two adjacent bond vectors) as a function of temperature (T). (f–i) R, contour length of primitive path (L_{pp}), Kuhn length of primitive path (R^2/L_{pp}), and entanglement length (N_e) vs C_∞^*. Here, the reduced temperature unit is 1 = 550 K, and the reduced time unit is estimated as 1–3.5 ps by Rouse relaxation time at T = 1.0. The time step is dt = 0.01 (~35 fs). Periodic boundary condition and NPT ensemble (at 1 atm) are applied. The simulated system consists of 1000 chains and each chain has 1000 repeat units. The initial conformation is generated by self-avoiding random walk relaxed over 8 × 10^7 time steps (~2800 ns) at T = 1.0 and 0.9. The rates of continuous cooling (T = 0.9 to 0.75), heating (T = 0.75 to 0.93), and recooling (T = 0.93 to 0.75) are the same and correspond to 2 × 10^{-7} (~0.031 K/ns). The crystallization is indicated by the dashed vertical lines. The final crystallinities at T = 0.75 are about 41.7 and 39.4% for cooling and recooling, respectively. All values shown in this figure are statistically averaged for all chains.

entanglement can be related with each instantaneous polymer conformation. However, for linear chains such a topological state is a priori not well-defined. One way to solve this problem, at least in computer simulations, is to perform PPA. Here, for each configuration in a MD trajectory, intrachain repulsions are switched off, followed by energy minimization to a local minimum with fixed chain ends.[11,18] To analyze the degree of entanglement of a given chain, the entanglement length (N_e) of the resulting primitive path is calculated. In this work we are interested in local entanglement properties that can vary even within a given chain. Therefore, the N_e used in this work is defined by the number of monomers in a kink-to-kink segment in the final structure after PPA,[18] as described in Figure 3a.

The evolution of N_e during the cooling/heating cycles is shown in Figure 1b. Before the onset of crystallization, the values of N_e at the same T show significant difference between cooling and recooling, while specific volumes and energies are nearly the same. In Figure 1c–e, we show the changes of radius of gyration (R_g), end-to-end distance (R), and the effective persistence length (C_∞^*). The configurations of polymers in melt state are randomly coiled, but slightly deviated from ideal Gaussian chains, where $R/\sqrt{6} = R_g$ holds. The persistence length, C_∞^*, increases steadily during cooling which leads to the increase of R and R_g.

During cooling in amorphous state, N_e decreases. This is consistent with previous simulations and theoretical models, and is caused by the increase of stiffness, C_∞^*, which leads to an increase of the contour length of PP (L_{pp}) and a weak decrease of Kuhn length of PP ($a_{pp} = R^2/L_{pp}$),[18−20] related with a decrease in N_e. In our case, the system is in a weakly entangled state,[21] and N_e as defined here can be considered as a measure of the number of monomers per Kuhn length of the PP. In Figure 1f–h, we display R, L_{pp}, and R^2/L_{pp} as a function of C_∞^*. Our results suggest a nearly constant value of $a_{pp} \cong 8$. Assuming Gaussian statistics between two entanglement points we obtain $N_e \sim 1/C_\infty^*$, a relation that is in good agreement with our results in the regime of $C_\infty^* < 6$ ($T > 0.85$), see Figure 1i. The reduced tube thinning, as compared to the expectation in literature, may be related with the nonequilibrium character of the chain conformations during cooling which leads to stretching of PP but not yet to full reentanglement. We mention that the value of N_e given in this paper is directly calculated by the number of monomers in a kink-to-kink segment, but not based on Gassian statistics as reported in the original paper of PPA by Everaers et al.[11]

With the onset of crystallization, N_e increases rapidly, which indicates a disentanglement process. C_∞^* and R_g also increase rapidly near T_c, while the R even slightly decreases. The larger deviation between $R/\sqrt{6}$ and R_g is related with the formation of partially extended chain parts (stems) and folds, resulting in non-Gaussian conformations. The value of L_{pp} decreases, which corresponds to the formation of large "blobs" of unentangled monomers corresponding to the crystalline folds. In the crystalline regime, chain conformations and the statistics of PPs should not be assumed as Gaussian with constant step length. During postcrystallization ($T < 0.78$) and subsequent heating near to T = 0.88, N_e continuously increases, corresponding to an improvement of crystalline order.

During further heating, N_e drops rapidly after reaching T = 0.88, where the melting process starts. The thermodynamic signature of melting seizes at T = 0.90. The value of N_e continues to decrease with the increase of temperature up to T = 0.93 (~16.5 K above the melting point) due to slow relaxation of the topological state in melts. The re-entanglement saturates at about T = 0.93. The value of N_e after melting is lower than that of the melt before the first crystallization/melting cycle, which indicates a relaxation of the state of entanglement during the cycle. The melt before the first cooling sweep was not yet in the fully entangled state and this explains the higher crystallization temperature.

Continuous cooling/heating cycles are dominated by homogeneous nucleation and strong reorganization processes.[13] To obtain polymer crystallization dominated by growth of a single lamella self-seeding protocols can be applied. As reported previously,[14] self-seeding (T_s = 0.9006) followed by an isothermal quench (T_q = 0.85) leads to isothermal lamellar growth. It is interesting to note that T_s is located in the window between T = 0.9 (thermodynamic melting is completed) and T = 0.93 (reentanglement process saturates) reported above. During isothermal growth after self-seeding at T_q = 0.85, the overall crystallinity (χ) of the single lamella, and the averaged values of R_g, R, and C_∞^* increase monotonously, see Figure 2b,c. The small jump of C_∞^* at the beginning

dx.doi.org/10.1021/mz300552x | ACS Macro Lett. 2013, 2, 31−34

indicates the quick response of local chain properties after the quench.

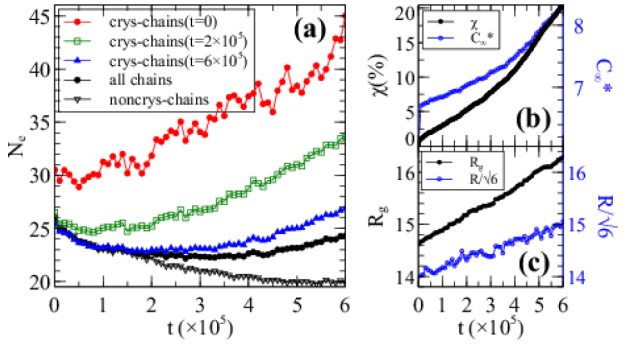

Figure 2. (a–c) Entanglement length (N_e) for selected chains, crystallinity (χ), effective persistent length (C_∞^*), radius of gyration (R_g), and end-to-end distance (R) vs quench time (t) during self-seeding at T = 0.85. Here, "crys-chains (t =)" means the chains are selected from the crystallized part at a certain time, and "noncrys-chains" means the uncrystallized chains until $t = 6 \times 10^5$.

In Figure 2a, we show N_e of different subsets of chains during lamellar growth. The value of N_e for all chains first decreases and then increases. The reason for this nonmonotonous behavior is the competition of disentanglement of crystallizing chains, and reentanglement of amorphous chains due to local stiffening. This can be verified by analyzing N_e for different sets of chains taken at different entry-time to the crystal. The value of N_e for chains involved in the initial seed, "crys-chains (t = 0)", monotonically increases, while that of noncrystallized chains, "noncrys-chains", monotonically decreases.

To follow the disentanglement process during crystallization we analyze the trajectory and entanglement state of a single chain. In Figure 3b,c, we show the changes of structures and primitive paths for two chains during continuous cooling and self-seeding respectively. As discussed in previous work,[12−14,22−24] the crystallization of polymer chains is via the emerging and developing of folds. The folds (in crystalline states) are considered to be unentangled, which can be partially verified in Figure 3b,c. A fold is created preferentially in a chain part which belongs to a very high value of N_e, both for homogeneous nucleation and self-seeding (growth).

In Figure 3d, we compare the local value of N_e and the stem length, d, during self-seeding. It is found that the images of monomers colored by value of N_e show correct location of the crystalline lamella inside which the value of N_e is larger (less entangled). The N_e images also show that the surface of lamella is disentangled which mainly consists of bending loops of folds. We note that clusters with higher value of N_e around the initial seed at t = 0 correspond to the just molten segments during the heating before self-seeding. These segments rest in less entangled states after melting indicating that reentanglement is slow as compared to the self-seeding time we have chosen. The retarded reentanglement of just molten chains leads to the increase of R during growth which is in contrast to the slight decrease during continuous cooling, see Figure 2d. We conclude that PPA reveals a crucial role of local entanglement properties for both nucleation and growth, which can be related to the memory effects found in experiments of self-nucleation.[9,10]

Another way to follow entangled dynamics is to analyze the trajectory of a chain in time. We visualize the trajectories of two chains in Figure 3e,f, from which we can see the formation of folds during crystallization. In the melt state, the movement of a chain is confined within a tube. However, there are some long unentangled segments in melts which play an important role in the early stage of crystallization, especially for homogeneous

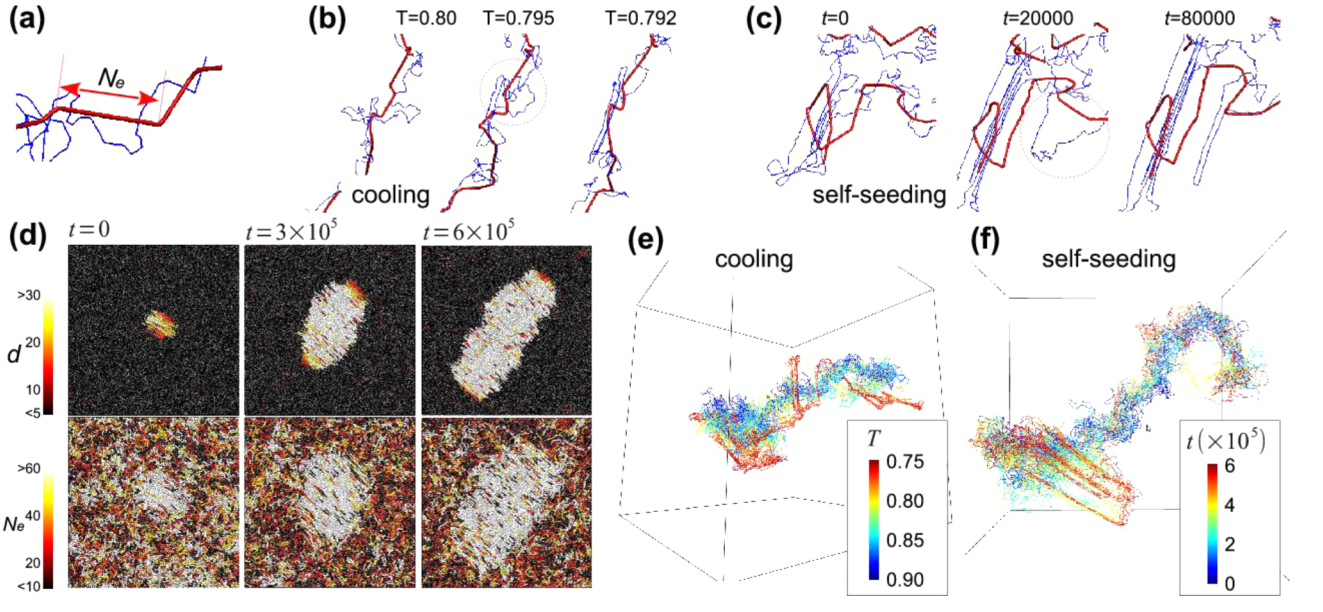

Figure 3. (a) Sketch of entanglement length (N_e or called primitive step) by the number of monomers between two nearby kinks of a Primitive Path (PP). The blue thin lines are the real configuration and the red thick lines are the PP given by PPA. (b, c) Configurations and PPs of two chains during cooling and self-seeding. The corresponding temperature (T) and quench time (t) are given in the top of the images. Red circles highlight the emerging of folds which signals the beginning of crystallization of certain segments. (d) Section view of stem length, d, and N_e during self-seeding. The corresponding color maps and time are shown in the left and top of the images, respectively. For the N_e view of each monomer, we use their real coordinates but colored by its corresponding value of N_e. (e, f) Colored trajectories of a chain during continuous cooling and self-seeding, respectively. The different colors are according to different temperature (T) or quenching time (t), as shown in the color maps.

dx.doi.org/10.1021/mz300552x | ACS Macro Lett. 2013, 2, 31−34

nucleation. The emerging and development of folds are very quick compared to the relaxation of entanglement. They are highly restricted by the local entanglement state and prefer unentangled segments. In Figure 4, we monitor the

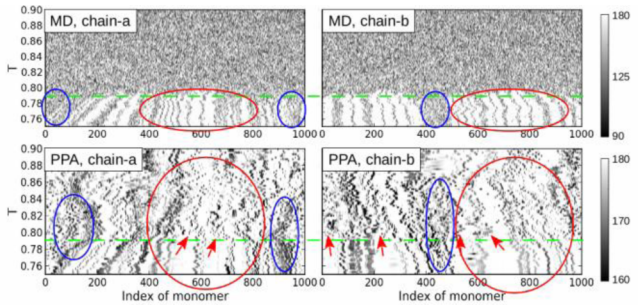

Figure 4. Angle values of two typical chains during continuous cooling calculated by normal MD trajectories (upper panels) and PPA conformations (lower panels). The corresponding color maps are shown at the right. Here the green dashed lines indicate the apparent crystallization temperature $T_c = 0.79$. Higher values of angle mean the corresponding segments are straight. Thus the "white belts" in the upper panels correspond to crystallized stems, and the "dark lines" in the lower panels correspond to kinks in primitive paths. The blue ellipses mark the regions with higher entanglement while the red ones mark the regions with lower entanglement. The red arrows mark the vanishing of PPA-kinks due to crystallization.

disentanglement process during continuous cooling by comparing the angular values of MD trajectories and PPA conformations. At the onset of crystallization, $T \sim 0.8$, some folds emerge and some PPA-kinks vanish (marked by red arrows in Figure 4). The vanishing of PPA-kinks may be related to the sliding motion as shown in our previous work.[14] Moreover, from Figure 4, we can see the folds emerge at where segments are less entangled (marked by red ellipses) and the segments with higher entanglement finally result in uncrystallized coils (marked by blue ellipses). We note that the longer unentangled segments already exist in melt state and are not due to the crystallization. Thus there is a strong correlation between the early stage of crystallization and entanglement state, which can be a clue to answer a classic question in polymer crystallization: Where will a crystalline seed appear and why?

We conclude that topological analysis based on primitive paths reveals disentanglement processes during crystallization. This competes with tightening of entanglement constraints during cooling caused by local stiffening of chains. The Kuhn length of the primitive path coincides with the stem length developed in the crystalline state and a lower entanglement density in the melt leads to an increase of the crystallization temperature. This might point to a significant role of entanglements for the crystallization from melt state. We also found indications that exceptionally large unentangled sequences are involved in homogeneous nucleation. This may be the reason of why homogeneous nucleation is strongly dependent on the thermal history of a sample. The topological analysis also reveals a possible origin of memory effect found in self-nucleation experiments. The effect of entanglement to crystallization behavior could be verified in experiments by measuring the deviation of crystallization temperatures for different initial samples, and should be helpful to thermodynamic theories[25] to improve the understanding of entanglement related primary nucleation.

AUTHOR INFORMATION

Corresponding Author

*E-mail: luo@ipfdd.de.

Notes

The authors declare no competing financial interest.

ACKNOWLEDGMENTS

We gratefully acknowledge financial support by the DFG (SO 277/6-2) and we thank ZIH der TU Dresden for computing time.

REFERENCES

(1) Strobl, G. *The Physics of Polymers*, 3rd ed.; Springer: Berlin, 2007.
(2) Strobl, G. *Rev. Mod. Phys.* **2009**, *81*, 1287.
(3) Muthukumar, M. *Adv. Polym. Sci.* **2005**, *191*, 241−274.
(4) Olmsted, P. D.; Poon, W. C. K.; McLeish, T. C. B.; Terrill, N. J.; Ryan, A. J. *Phys. Rev. Lett.* **1998**, *81*, 373−376.
(5) Hoffman, J. D. *Polym. Eng. Sci.* **1964**, *4*, 315−362.
(6) DiMarzio, E. A.; Guttman, C. M.; Hoffman, J. D. *Faraday Discuss. Chem. Soc.* **1979**, *68*, 210−217.
(7) Rastogi, S.; Lippits, D. R.; Ppeters, G. W. M.; Graf, R.; Yao, Y.; Spiess, H. W. *Nat. Mater.* **2005**, *4*, 635−641.
(8) Lippits, D. R.; Rastogi, S.; Talebi, S.; Bailly, C. *Macromolecules* **2006**, *39*, 8882−8885.
(9) Mamun, A.; Umemoto, S.; Okui, N.; Ishiharar, N. *Macromolecules* **2007**, *40*, 6269.
(10) Xu, J.-J.; Ma, Y.; Hu, W.; Rehahn, M.; Reiter, G. *Nat. Mater.* **2009**, *8*, 348−353.
(11) Everaers, R.; Sukumaran, S. K.; Grest, G. S.; Svaneborg, C.; Sivasubramanian, A.; Kremer, K. *Science* **2004**, *303*, 823−826.
(12) Meyer, H.; Müller-Plathe, F. *Macromolecules* **2002**, *35*, 1241−1252.
(13) Luo, C.; Sommer, J.-U. *Phys. Rev. Lett.* **2009**, *102*, 147801.
(14) Luo, C.; Sommer, J.-U. *Macromolecules* **2011**, *44*, 1523−1529.
(15) Plimpton, S. *J. Chem. Phys.* **1995**, *177*, 1−9.
(16) Luo, C.; Sommer, J.-U. *Comput. Phys. Commun.* **2009**, *180*, 1382−1391.
(17) Yu, X.; Kong, B.; Yang, X. *Macromolecules* **2008**, *41*, 6733−6740.
(18) Foteinopoulou, K.; Karayiannis, N. C.; Mavrantzas, V. G.; Kroger, M. *Macromolecules* **2006**, *39*, 4207−4216.
(19) Sukumaran, S. K.; Grest, G. S.; Kremer, K.; Everaers, R. *J. Polym. Sci., Part B: Polym. Phys.* **2005**, *43*, 917−933.
(20) Hoy, R. S.; Robbins, M. O. *J. Polym. Sci., Part B: Polym. Phys.* **2006**, *44*, 3487−3500.
(21) Uchida, N.; Grest, G. S.; Everaers, R. *J. Chem. Phys.* **2008**, *128*, 044902.
(22) Hu, W.; Frenkel, D.; Mathot, V. B. F. *Macromolecules* **2003**, *36*, 8178−8183.
(23) Yamamoto, T. *J. Chem. Phys.* **2008**, *129*, 184903.
(24) Gee, R. H.; Lacevic, N. M.; Fried, L. E. *Nat. Mater.* **2006**, *5*, 39−43.
(25) Milner, S. T. *Soft Matter* **2010**, *7*, 2909−2917.